Magnitude estimation for early warning applications using the initial part of P waves: A case study on the 2008 Wenchuan sequence

Weitao Wang,[1] Sidao Ni,[1] Yong Chen,[1] and Hiroo Kanamori[2]

Received 13 April 2009; revised 23 June 2009; accepted 24 July 2009; published 27 August 2009.

[1] A period parameter τ_c and an amplitude parameter Pd determined from the very beginning of P wave are important for earthquake early warning (EEW), yet their dependence on source mechanism, focal depth and epicentral distance has not been fully studied. After the devastating Mw7.9 Wenchuan earthquake, hundreds of M4-6 earthquakes occurred with diverse focal mechanisms and depth range of 2–20 km. We calculate τ_c and Pd of these aftershocks and examine their dependence on magnitude, τ_c, distance, and depth. We find that τ_c correlates well with magnitude, but joint regression including distance and depth does not significantly improve the correlation. The effect of focal mechanism on the τ_c -magnitude correlation is not obvious. When P wave is nodal, τ_c measurement becomes inaccurate. Also, τ_c is systematically greater for slow earthquakes, leading to a possible false alarm. Thus, more studies are required to discriminate slow earthquakes for robust early warning.
Citation: Wang, W., S. Ni, Y. Chen, and H. Kanamori (2009), Magnitude estimation for early warning applications using the initial part of P waves: A case study on the 2008 Wenchuan sequence, *Geophys. Res. Lett.*, *36*, L16305, doi:10.1029/2009GL038678.

1. Introduction

[2] Earthquake Early Warning System (EEWS) provides alerts to urban areas near the epicenter so that appropriate measures against strong ground shaking can be taken. Early warning information can be used for personal protection, e.g., people at home or in the workplace can hide in safer sites and move away from dangerous chemicals and machinery. Institutional uses of short-term warnings include automated mass-transportation systems that can utilize a few seconds to slow down trains, abort airplane landings, and prevent additional cars from entering a freeway. Industries can initiate shutting down processes for critical facilities before peak ground motion arrives, preventing cascading failures [*Kanamori*, 2005]. Early warning of strong aftershocks is also very helpful. Clean-up personnel working on unstable debris can move to a safe place. *Bakun et al.* [1994] describe such a system to protect construction workers from hazard during the aftershock sequence of the 1989 Loma Prieta earthquake. In the past decades, substantial progress has been made to turn EEW into practical implementation [*Nakamura*, 1988; *Espinosa-Aranda et al.*, 1995; *Wu et al.*, 1998; *Wu and Teng*, 2002; *Horiuchi et al.*, 2005]. In EEW studies, period parameters such as τ_c are among the most important for rapid estimation of earthquake magnitude [*Nakamura*, 1988; *Kanamori*, 2005; *Wu et al.*, 2006; *Wu and Kanamori*, 2008]. Although many studies have demonstrated that τ_c is a simple yet useful estimator of magnitude, there are several unresolved issues [*Yamada and Ide*, 2008; *Wolfe*, 2006]. *Olson and Allen* [2005] argue that the first few seconds after the P arrival can partially control the eventual magnitude of the event. Although period parameters like τ_c have been widely used, the influence of epicentral distance, focal depth, focal mechanism or rupture velocity has not been systematically investigated yet because of the limited data available for such studies.

[3] After the Mw7.9 Wenchuan earthquake on May 12, 2008, hundreds of aftershocks with magnitudes ranging from 4 to 6 occurred over a rupture length of about 300 km with focal depths from 2 to 20 km. By 29 August 2008, a total of 261 aftershocks with magnitudes larger than 4.0 occurred according to the Chinese National Seismic Network; among them 39 aftershocks were larger than 5.0 and 8 aftershocks, larger than 6.0. The largest aftershock occurred on 25 May with a magnitude 6.4 with strike slip mechanism at a depth of 18 km near the northeastern end of the rupture. Aftershocks in the northeastern segment have diverse mechanisms, and a wide range of focal depth (2–20 km) [*Zheng et al.*, 2009b]; this activity, if migrated beyond the northeastern end of the rupture zone, poses additional seismic hazard in the area.

[4] In this paper, we first calculate τ_c for the well recorded aftershocks in the northeastern segment, perform linear regression of τ_c on magnitude to determine the empirical relationship between τ_c and magnitude. For this regression, we use the average of τ_c over multiple stations. Also, by using τ_c values obtained from single stations, we make a joint linear regression on τ_c, magnitude, focal depth, and epicentral distance to examine the influence of these parameters on the magnitude estimation. An amplitude parameter Pd is also calculated. For the aftershocks, we only choose the events in the northeastern segment of the rupture zone for several reasons. (1) There are more permanent stations in the north; furthermore a large number of portable instruments were deployed to record the aftershocks. (2) Many large aftershocks occurred in the northeastern segment through September, 2008. (3) The aftershocks in the northeastern segment show diverse focal depth and mechanism. Thus, many records were obtained for the aftershocks which provided us with basic data for making systematic investigations on the relationship

[1] Mengcheng National Geophysical Observatory, School of Earthquake and Space Science, University of Science and Technology of China, Hefei, China.
[2] Seismological Laboratory, California Institute of Technology, Pasadena, California, USA.

0094-8276/09/2009GL038678$05.00

Table 1. List of Events Studied in This Paper[a]

Event Date	Time	Longitude	Latitude	Centroid Depth (km)	Magnitude	Number of Records	Remark
2008/05/12	06:28:01	103.3	31.0	13.0	7.9	21	10 accelergrams
2008/05/19	04:08:58	105.0	32.1	16.0	4.8	10	
2008/05/19	06:06:54	105.3	32.5	6.0	5.4	12	
2008/05/19	17:52:36	104.9	32.3	12.0	5.0	12	
2008/05/20	03:42:28	105.4	32.6	10.0	4.0	11	
2008/05/21	09:33:13	105.2	32.3	11.0	4.5	10	
2008/05/22	11:22:27	105.4	32.6	19.0	4.0	7	
2008/05/25	09:21:46	105.4	32.6	19.0	6.1	13	
2008/05/27	08:03:24	105.6	32.7	15.0	5.4	11	
2008/05/27	08:37:53	105.6	32.8	14.0	5.7	11	
2008/05/27	13:59:36	105.2	32.5	13.0	4.7	12	
2008/05/27	17:35:11	105.4	32.7	11.0	4.7	10	
2008/05/31	06:22:42	105.0	32.4	16.0	4.0	10	
2008/06/05	04:41:08	105.0	32.3	17.0	5.0	15	
2008/06/05	06:02:32	105.5	32.7	9.0	4.3	15	
2008/06/07	06:28:34	105.4	32.5	16.0	4.3	15	
2008/06/07	07:32:47	105.2	32.5	12.0	4.0	15	
2008/06/10	16:27:28	105.8	32.8	16.0	4.3	12	
2008/06/17	05:51:44	105.6	32.8	19.0	4.5	14	
2008/06/17	13:40:46	104.9	32.3	16.0	4.0	17	
2008/06/19	10:25:58	105.5	32.8	8.0	4.4	13	
2008/07/23	19:54:45	105.5	32.8	2.0	5.5	15	
2008/07/24	07:09:30	105.5	32.8	11.0	5.7	14	
2008/08/01	08:32:43	104.7	32.0	16.0	5.7	15	
2008/08/05	09:49:17	105.5	32.8	2.0	6.0	14	

[a]Data provided by CSNDMC. See *Zheng et al.* [2009a] for information of data availability.

between predominant period and the magnitude. In contrast, many stations around the southwestern segment malfunctioned due to damage caused by the mainshock in the first two weeks; all the large aftershocks in the southwestern segment occurred during this period.

2. Data and Analysis

[5] In this paper, we chose the mainshock and 24 aftershocks before August 05 in the northeastern segment for investigation. Each of the aftershocks was well recorded by at least 7 stations within a distance of 100 km from epicenter. For the main shock, we have 4 broad-band velocity records from the permanent stations and 10 strong motion acceleration records within 100 km from the epicenter. The sampling rates are 50 samples per second for the broad-band velocity records and 100 samples per second for strong motion accelerograms. In total, we used 324 waveforms with good quality for the mainshock and aftershocks in this study (Table 1). The spatial distribution of the events and stations are shown in Figure 1. Acceleration records are converted to velocity records, and velocity records to displacement records, since velocity and displacement seismograms are needed for τ_c calculation. Following the procedure of *Wu and Kanamori* [2008], we apply a 0.075 Hz high-pass Butterworth filter on the vertical component of ground-motion displacement to remove the drift of the displacement, then calculate the two parameters τ_c and Pd using the first 3 s after the arrival of P wave. And τ_c is defined as: $\tau_c = 2\pi/\sqrt{r}$ and $r = \int_0^{\tau_0} \dot{u}^2 dt / \int_0^{\tau_0} u^2 dt$.

[6] Here u is the high-pass filtered displacement of the vertical component ground motion, and $\dot{u}$ is the velocity record. τ_0 is the duration over which we calculate the τ_c parameter; here $\tau_0 = 3$ s is used. τ_c approximately represents the P wave pulse width and is found to correlate with magnitude [*Kanamori*, 2005]. Pd is the maximum displacement amplitude during the same time window. *Wu and Kanamori* [2005b] showed that Pd can be used to estimate the peak ground motion velocity (PGV) at the same site. τ_c and Pd have been demonstrated to be useful for early

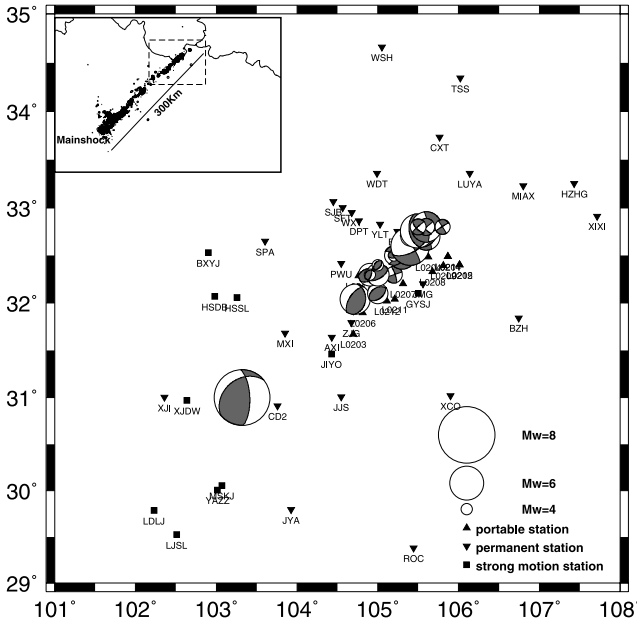

Figure 1. Map of broadband stations (permanent stations as inverted triangles, and portable stations as triangles) and events used in this study. The events are shown with the mechanism diagram with its size proportional to the magnitude. A sketch indicating the rupture area and event distribution is shown in the upper left inset. The main shock is indicated as solid black star. Only the aftershocks in the northeastern segment of the rupture zone (in dashed rectangle) are studied because of diversity of focal depth, mechanism and good station coverage.

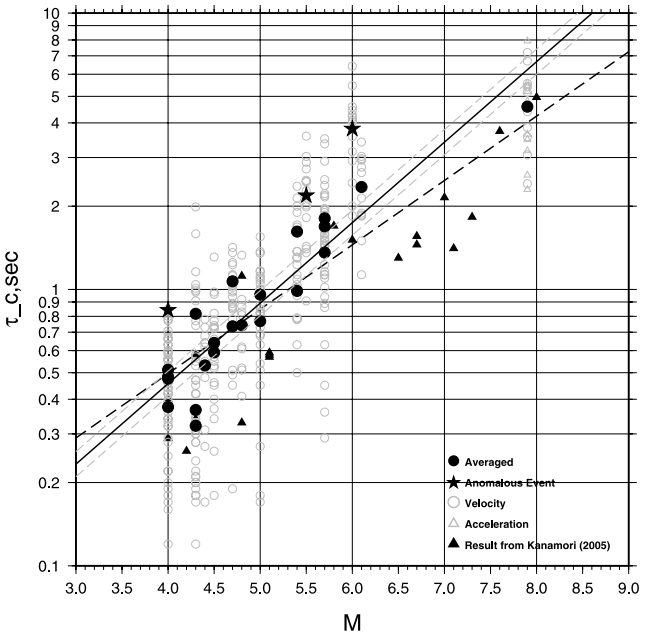

Figure 2. τ_c calculated from the first 3 s of P wave (open gray circles from single broad-band velocity record, and open gray triangles for strong motion records, solid black circles for averaged τ_c, solid black stars for the three anomalous τ_c values) The empirical τ_c vs. magnitude relation determined by our study is shown by black solid line with its standard deviations shown by gray dashed lines. The result from *Kanamori* [2005] is shown by black dashed line as comparison.

warning, either in multiple station approach or single station approach [*Wu et al.*, 2006]

2.1. Multiple Station Approach for τ_c

[7] The automatic P first arrival picking method described by *Allen* [1978] is used to detect the P arrival from the vertical record. Since accurate τ_c estimation depends highly on the correct detection of P arrival [*Kanamori*, 2005], we double check the arrival time by visual inspection of the waveforms. For most records automatic timing is precise, but we make manual picks on several records where P first arrival can not be detected by the automatic method due to inferior waveform quality. Figure 2 displays τ_c for all the events obtained from both broad-band velocity records and strong motion acceleration records. τ_c obtained from each broad-band record is shown by gray open circles, and strong motion record, by gray open triangles. We averaged τ_c over a few stations for each event to obtain more robust estimations; the average τ_c's are shown by solid black circles in Figure 2. The τ_c values calculated for large earthquakes in Japan, Taiwan, and southern California [*Kanamori*, 2005] are also shown as solid black triangles for comparison.

[8] For the mainshock, both broad-band velocity records and strong motion acceleration records give consistent estimations. The average of τ_c for the main shock is about 4.6 s, and would approximately correspond to M = 8. Similar to the results in the previous studies, τ_c generally increases with magnitude, suggesting that τ_c is a useful parameter for magnitude estimation in early warning systems. However, we also notice three anomalous averaged τ_c values which are well above the regression line. This means that if these τ_c values are used for magnitude estimation, the magnitudes will be overestimated and may result in false alarms in practical operations. We make further investigations on these three anomalous events. For the first anomalous M4.0 event, we notice that normal τ_c values are obtained from 6 records while 2 extremely large values are obtained from the other two records. The spatial distribution of the stations for this event is shown in Figure 3a, together with the τ_c values and the source mechanisms. Figure 3a shows that the stations giving anomalously large τ_c values lie close to the nodal plane of the earthquake.

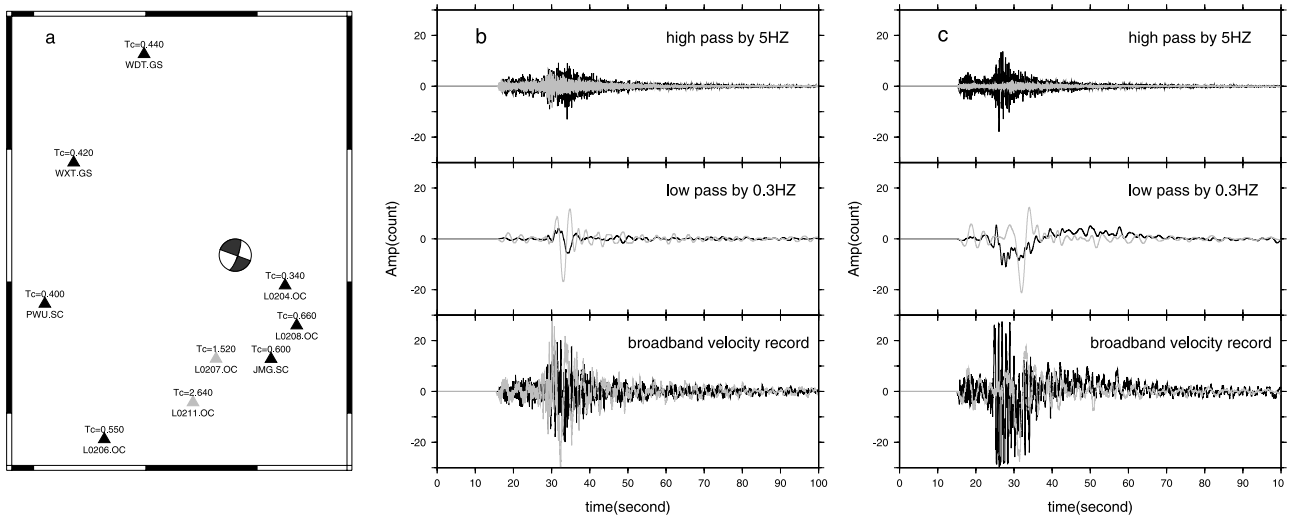

Figure 3. Three anomalous events with large τ_c values. (a) The anomalous M4.0 event with the focal mechanism. τ_c values determined from each station are marked above the station. The station used are shown by triangles while normal τ_c estimation filled with black and overestimation, filled with gray. (b) The anomalous M5.5 event. The waveforms of the anomalous events are shown in gray, while the waveforms of a nearby normal earthquake in black. (c) The anomalous M6.0 event. Events in Figur es 3b and 3c show less high frequency energy, suggesting slower rupture.

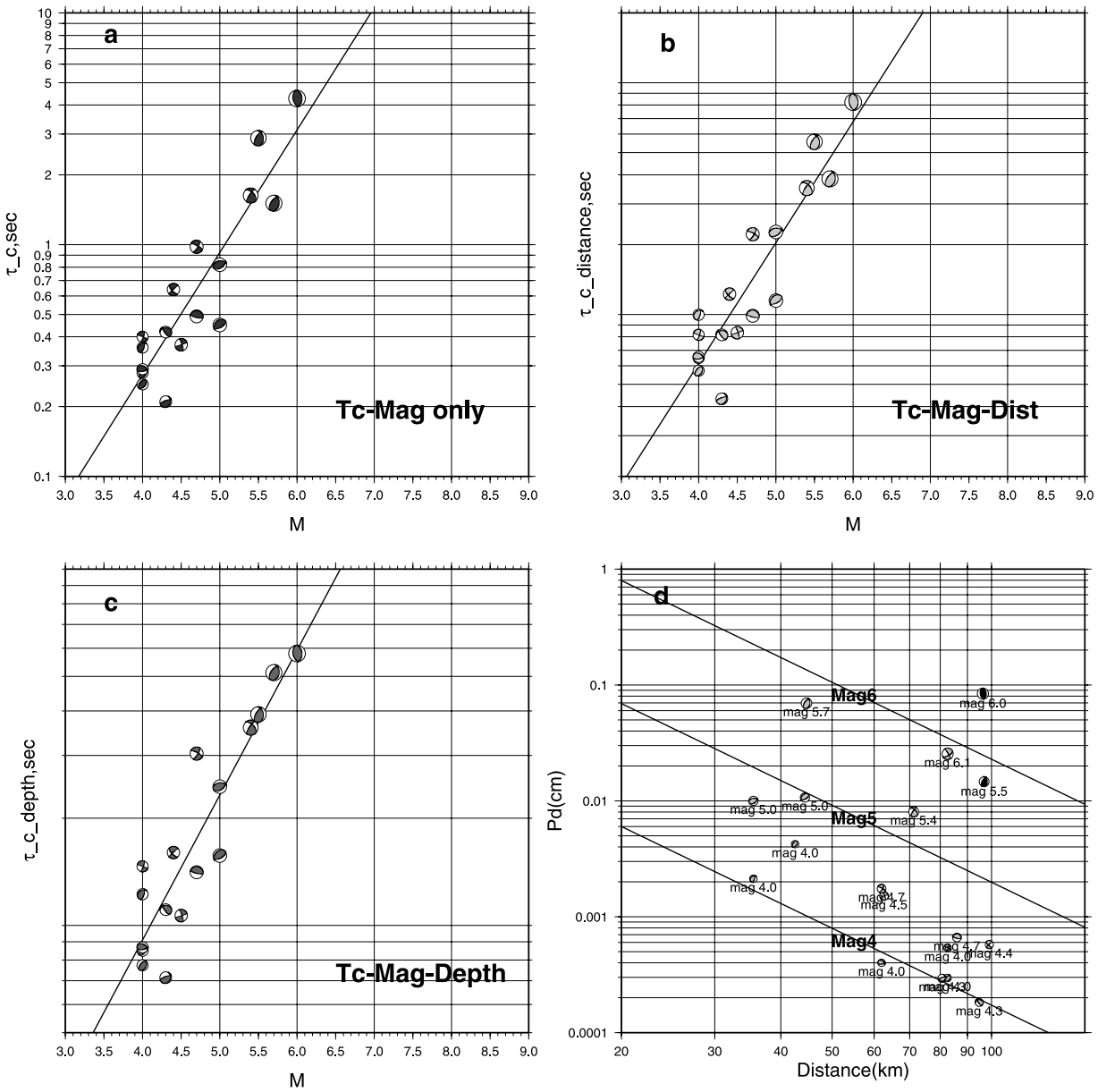

Figure 4. (a) τ_c estimation using just one station (PWU). (b) The effects of distance on τ_c is modeled with a linear relation of $\tau_c = A\ LogM + B\ Log(distance) + C$ via regression. τ_c _distance = $\tau_c - B\ log(distance)$ *vs. M* is plotted to show whether the effects of distance can be taken into account to reduce scatters. (c) The effects of depth on τ_c is modeled with $\tau_c = D\ LogM + E\ Log(depth) + F$ via regression. τ_c _depth = $\tau_c - E\ log(depth)$ is plotted vs *M*. (d) Pd obtained from the data at PWU station.

[9] For the other two anomalous events, the τ_c values are systematically high for all the stations regardless of the azimuth. Since τ_c is a measure of the predominant period, we suspect that these two events may have unusual spectra, and investigate the waveforms in three different frequency bands (broadband, long period band with a period of 3 s or longer, and high frequency band with 5 Hz or higher). As shown in Table 1, these two events are shallow with a focal depth around 2 km. For each of the two events, we choose a normal event (with τ_c close to the regression line) and compare their amplitude in the three frequency bands. From Figures 3b and 3c, we observe that the two anomalous earthquakes (gray waveforms) have strong low frequency component but weak high frequency component compared to normal events (black waveforms). Thus, these two shallow events have characters of slow earthquakes and the dominant longer period components yield large τ_c. Since a large τ_c may lead to a false alarm, special attention should be paid to earthquakes with anomalous spectrum.

[10] Excluding the three anomalous events, we perform a linear regression using the averaged τ_c values and magnitudes. The empirical relation $\log(\tau_c) = 0.291 * M - 1.506 \pm 0.011$ is shown by solid black line in Figure 2,the dashed gray lines indicate the standard deviation. We compare our result with the relation obtained for large earthquakes from Japan, Taiwan, and southern California [*Kanamori*, 2005], shown by dashed black line in Figure 2. The slope is slightly different but both show a good correlation between

τ_c and magnitude. This suggests that τ_c is useful for early warning purposes in the Sichuan area in China.

2.2. Single Station Approach

[11] Usually τ_c shows a fairly large scatter for an event recorded at different stations, and average of τ_c over many stations is used for magnitude estimation [*Wu and Kanamori*, 2005a; *Wu et al.*, 2007; *Wu and Kanamori*, 2008]. However, recent studies demonstrate that τ_c from only one station can also provide a fairly good estimate of magnitude [*Wu et al.*, 2006]. Although many studies have been made on the relation between τ_c and magnitude, not much has been done to investigate the influence of the epicentral distance and focal depth on the τ_c vs. magnitude relationship. We made a joint regression on the distance and depth respectively for PWU station (Figure 4). We first model the effects of distance on τ_c by fitting a linear relation of τ_c = A LogM + B Log(distance) + C, then model the effects of depth with τ_c = D LogM + E Log(distance) + F. If τ_c depends on distance, then the plot of τ_c − B log(distance) vs. M would reduce scatter as compared to the plot of τ_c vs. M. However, in Figure 4b, we do not observe substantial improvement in reducing scatter, therefore τ_c is a good indicator of source strength and does not depend on the epicentral distance within 100 km [*Wu et al.*, 2007]. The situation is similar for the effects of depth (Figure 4c), where τ_c − E log(depth) is plotted vs M. The result shows that neither the distance joint regression nor the focal depth joint regression makes substantial improvement. This demonstrates that the focal depth and epicentral distance do not play an important role in magnitude estimation using the τ_c method. Of course, the depth range of the Wenchuan sequence is limited in the upper crust, and may not be large enough to show the effects on regression. In Japan where subduction-zone earthquakes are frequent the depth range is larger and τ_c of deep events may not necessarily be similar to that of shallow earthquakes with similar magnitudes. The mechanism does not seem to play a significant role either, as the data points for both strike-slip and thrust earthquakes scatter around the regression line in a similar way (Figure 4a). We also calculate Pd for 16 events recorded at PWU station. The result agrees with that obtained by *Wu and Zhao* [2006] and *Wu et al.* [2007] in both Taiwan and southern California, where a relation $log(Pd) = A + B\ M + C\ Log\ (distance)$ is adopted in regressing Pd with magnitude and distance. This suggests that even with one station, τ_c and Pd can be used to obtain reasonable estimates of magnitude, after preliminary location is available. Such location is obtainable even with a single station or with more stations in an incremental way [*Odaka et al.*, 2003; *Horiuchi et al.*, 2005].

3. Discussion and Conclusion

[12] We calculated τ_c and Pd for the Wenchuan Mw7.9 mainshock and 24 aftershocks in the northeastern segment of the rupture zone. The waveforms we use include broadband velocity records from both permanent and portable stations, as well as accelerograms from strong motion stations. The source mechanisms of these events vary from thrust to strike slip, with a magnitude range from M4 to M8 and focal depth from 2 to 20 km. The diversity of the source provides us with a good dataset for detailed investigation on the dependency of τ_c on the source mechanism, focal depth and epicentral distance.

[13] The result is overall consistent with those obtained earlier for earthquakes in Japan, southern California, and Taiwan. The slope of τ_c vs. magnitude relation is slightly different from that for Japan, southern California and Taiwan. The difference may be caused by the tectonic differences, as Japan, Southern California and Taiwan are located in the regions with short earthquake recurrence times, while the Wenchuan earthquake occurred in a region with long recurrence times [*Burchfiel et al.*, 2008]. The focal mechanism appears to have no substantial effect on τ_c estimation, which is good for early warning purposes because alarms can be issued without knowledge of the focal mechanism of the source. However, we also notice that slow earthquakes which have enhanced low frequency components may cause overestimates of τ_c leading to a false alarm. This problem needs to be further investigated for practical implementation.

[14] We tested a single station approach because it is useful for early warning in those areas with sparse stations. The results show that a single station is in general capable of providing useful estimates of earthquake magnitude. The slope of the τ_c vs magnitude regression line is different between single station and multiple station methods because of the site effects or propagation effects, but in both cases τ_c and magnitude correlate well. However, when a station is close to the P-wave nodal plane of the event, τ_c is often overestimated leading to a false alarm. We also make a joint regression to examine the effect of epicentral distance and the focal depth. The results suggest that neither the distance nor the focal depth has substantial effect on the magnitude estimation. This is good for early warning purposes because we need not worry about the focal depth of the earthquake and the epicentral distance, which are hard to determine accurately in 3 s after the earthquake occurred. The result of the Pd investigation is in good agreement with that of *Wu and Zhao* [2006].

[15] As shown in this paper and many other papers, τ_c and Pd can provide a quick estimation of the magnitude and ground-motion amplitude and are among the most important parameters for early warning systems.

[16] **Acknowledgments.** This research was supported by CAS funding and NSFC 40676073 and NSFC 40604004. Also supported by NSF, USGS contribution 2009-002, Menghceng National Geophysical Observatory. We also thank *Data Management Centre of China National Seismic Network at Institute of Geophysics, China Earthquake Administration* for providing the seismograms.

References

Allen, R. V. (1978), Automatic earthquake recognition and timing from single traces, *Bull. Seismol. Soc. Am.*, *68*, 1521–1532.

Bakun, W. H., F. G. Fischer, E. G. Jensen, and J. Van-Schaack (1994), Early warning system for aftershocks, *Bull. Seismol. Soc. Am.*, *84*, 359–365.

Burchfiel, B. C., et al. (2008), A geological and geophysical context for the Wenchuan earthquake of 12 May 2008, Sichuan, People's Republic of China, *GSA Today*, *18*(7), 4–11, doi:10.1130/GSATG18A.1.

Espinosa-Aranda, J., A. Jiménez, G. Ibarrola, F. Alcantar, A. Aguilar, M. Inostroza, and S. Maldonado (1995), Mexico City seismic alert system, *Seismol. Res. Lett.*, *66*, 42–53.

Horiuchi, S., H. Negishi, K. Abe, A. Kamimura, and Y. Fujinawa (2005), An automatic processing system for broadcasting earthquake alarms, *Bull. Seismol. Soc. Am.*, *95*, 708–718, doi:10.1785/0120030133.

Kanamori, H. (2005), Real-time seismology and earthquake damage mitigation, *Annu. Rev. Earth Planet. Sci.*, *33*, 195–214, doi:10.1146/annurev.earth.33.092203.122626.

Nakamura, Y. (1988), On the urgent earthquake detection and alarm system (UrEDAS), in *Proceedings of the Ninth World Conference on Earthquake Engineering*, vol. VII, pp. 673–678, Balkema, Rotterdam, Netherlands.

Odaka, Y., K. Ashiya, S. Tsukada, S. Sato, K. Ohtake, and D. Nozaka (2003), A new method of quickly estimating epicentral distance and magnitude from a single seismic record, *Bull. Seismol. Soc. Am.*, *93*, 526–532, doi:10.1785/0120020008.

Olson, E. L., and R. M. Allen (2005), The deterministic nature of earthquake rupture, *Science*, *438*, 212–215.

Wolfe, C. J. (2006), On the properties of predominant-period estimators for earthquake early warning, *Bull. Seismol. Soc. Am.*, *96*, 1961–1965, doi:10.1785/0120060017.

Wu, Y. M., and H. Kanamori (2005a), Experiment on an onsite early warning method for the Taiwan early warning system, *Bull. Seismol. Soc. Am.*, *95*, 347–353, doi:10.1785/0120040097.

Wu, Y. M., and H. Kanamori (2005b), Rapid assessment of damaging potential of earthquakes in Taiwan from the beginning of P waves, *Bull. Seismol. Soc. Am.*, *95*, 1181–1185, doi:10.1785/0120040193.

Wu, Y. M., and H. Kanamori (2008), Exploring the feasibility of on-site earthquake early warning using close-in records of the 2007 Noto Hanto earthquake, *Earth Planets Space*, *60*, 155–160.

Wu, Y. M., and T. L. Teng (2002), A virtual sub-network approach to earthquake early warning, *Bull. Seismol. Soc. Am.*, *92*, 2008–2018, doi:10.1785/0120010217.

Wu, Y.-M., and L. Zhao (2006), Magnitude estimation using the first three seconds P-wave amplitude in earthquake early warning, *Geophys. Res. Lett.*, *33*, L16312, doi:10.1029/2006GL026871.

Wu, Y. M., H. Kanamori, R. Allen, and E. Hauksson (2007), Determination of earthquake early warning parameters, τc and Pd for southern California, *Geophys. J. Int.*, *170*, 711–717, doi:10.1111/j.1365-246X.2007.03430.x.

Wu, Y. M., T. C. Shin, and Y. B. Tsai (1998), Quick and reliable determination of magnitude for seismic early warning, *Bull. Seismol. Soc. Am.*, *88*, 1254–1259.

Wu, Y. M., H. Y. Yen, L. Zhao, B. S. Huang, and W. T. Liang (2006), Magnitude determination using initial P waves: A single-station approach, *Geophys. Res. Lett.*, *33*, L05306, doi:10.1029/2005GL025395.

Yamada, T., and S. Ide (2008), Limitation of the predominant period estimator for earthquake early warning and the initial rupture of earthquakes, *Bull. Seismol. Soc. Am.*, *98*, 2739–2745, doi:10.1785/0120080144.

Zheng, X. F., et al. (2009a), Technical system construction of Data Backup Centre for China Seismograph Network and the data support to researches on the Wenchuan earthquake (in Chinese), *Chin. J. Geophys.*, *52*(5), 1412–1417, doi:10.3969/j.issn.0001-5733.

Zheng, Y., H. Ma, J. Lv, S. Ni, Y. Li, and S. Wei (2009b), Source mechanism of strong aftershocks (M_s5.6) of the 2008/05/12 Wenchuan earthquake and the implication for seismotectonics, *Sci. China Ser. D*, *52*(6), 739–753, doi:10.1007/s11430-009-0074-3.

Y. Chen, S. Ni, and W. Wang, Mengcheng National Geophysical Observatory, School of Earthquake and Space Science, University of Science and Technology of China, Hefei, Anhui 230026, China. (sdni@ustc.edu.cn)

H. Kanamori, Seismological Laboratory, California Institute of Technology, 1200 East California Boulevard, Pasadena, CA 91125, USA.